

Improved Compact Modeling of Output Conductance and Cutoff Frequency of Bipolar Transistors

Jeroen C. J. Paasschens, Willy J. Kloosterman, Ramon J. Havens, and Henk C. de Graaff

Abstract—The collector epilayer is a crucial element in the behavior of modern bipolar transistors. Compact models for its description, like the Kull model, are therefore of crucial importance too. We give a Mextram-based improvement to these models for quasi-saturation and show that the output conductance and the cutoff frequency are less abrupt in this region. Apart from ohmic quasi-saturation, we also include quasi-saturation due to the Kirk effect, which results from velocity saturation.

Index Terms—Bipolar transistors, circuit simulation, compact modeling, distortion, high frequency, Mextram.

I. INTRODUCTION

THE SPICE–Gummel–Poon model is still the most widely used compact model to describe bipolar transistors, because of its simplicity. It is, however, well known that it cannot describe some of the effects that are important in modern bipolar transistors. One of the effects that is not adequately described is quasi-saturation. Quasi-saturation (i.e., the internal base–collector junction is forward biased, whereas externally it is reverse biased) degrades the performance of the transistor and is due to either ohmic voltage drop in the epilayer or to a voltage drop caused by velocity saturation (Kirk effect). Many improvements have been suggested over the years. One of the major contributions is the description of ohmic quasi-saturation by Kull *et al.* [1]. This epilayer model has been incorporated into, for instance, Mextram¹ [2], and Vbic² [3]. The physical basis of the model is sound. However, we will show that in its current implementations it has the disadvantage that it is not very smooth in first- and higher order derivatives of the current w.r.t. voltages.

We give an improvement to the Kull model that is much smoother. We also include velocity saturation, based on the same principles as in [2]. This results in a superior description of measurements. As an example, we compare to measurements on a high-voltage transistor in which the epilayer description is of crucial importance. This epilayer model will be part of the new Mextram 504 release, but it should be noted that it can be implemented in other models.

Manuscript received January 8, 2001; revised April 9, 2001.

J. C. J. Paasschens, W. J. Kloosterman, and R. J. Havens are with Philips Research Laboratories, 5656 AA Eindhoven, The Netherlands (e-mail: Jeroen.Paasschens@philips.com).

H. C. de Graaff is with Delft University of Technology, 2600 GB Delft, The Netherlands.

Publisher Item Identifier S 0018-9200(01)06110-8.

¹For the most recent model descriptions, source code, and documentation, see http://www.semiconductors.philips.com/Philips_Models

²For the model definition and more information about Vbic, see <http://www.fht-esslingen.de/institute/iaf/gp/neu/VBIC/index.html>

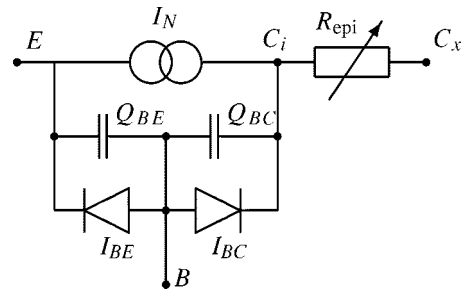


Fig. 1. The intrinsic part of the equivalent circuit of compact models like the Kull model, Vbic, and Mextram. We have not shown the extrinsic regions and all the resistances to the external terminals.

In Section II we start with the equivalent circuit of the intrinsic part of a bipolar transistor. We analyze the Kull model in Section III. In Section IV we show our improvements and the comparison with the Kull model. In Section V we add velocity saturation effects and the Kirk effect, while current spreading is shortly discussed in Section VI. Our experimental results are given in Section VII. In Section VIII, we describe the charge of the epilayer that is needed for the description of the cutoff frequency. Temperature scaling and parameter extraction are discussed in Sections IX and X. Convergence results on realistic circuits are given in Section XI, and, finally, we summarize in Section XII.

II. EQUIVALENT CIRCUIT OF COMPACT MODEL

Before we go to the model equations, we will first show the equivalent circuit used in many compact models for bipolar transistors. The intrinsic part of these equivalent circuits is shown in Fig. 1. It consists of base–emitter and base–collector diodes, a current source that describes both the forward and reverse main currents, and an element for the epilayer current. Furthermore, all modeled charges are shown as capacitances. The element for the epilayer current models the variable epilayer resistance (although in practice it is implemented as a current source). For low biases and current densities, its resistance is determined by the doping level of the epilayer³

$$R_{cv} = \frac{W_{epi}}{q\mu_n N_{epi} A_{em}} \quad (1)$$

where

W_{epi} the epilayer thickness;
 q the elementary charge;
 μ_n the (low-field) mobility;
 A_{em} the emitter area.

³Note that we use a special font to denote model parameters.

The given expression is for a 1-D model only and changes when current spreading needs to be considered. Also, the doping level of the epilayer N_{epi} is used in the expression. For the model derivation, we assume this doping level to be constant. In practice, it is of course an effective value.

The epilayer current depends on both the electron and hole densities in the epilayer. To model it, we need both the electron and hole quasi-Fermi levels. The epilayer current will therefore be given in terms of the voltage differences V_{BCi} and V_{BCx} , being the difference between the hole quasi-Fermi level in the base and the electron quasi-Fermi levels at the base–epilayer junction and at the interface between epilayer and buried layer.

III. ANALYSIS OF THE KULL MODEL

We start our analysis with the Kull model [1], before we give our improvements. The Kull model gives a good description of the currents and charges in the collector epilayer, as long as the whole epilayer is quasi-neutral. Quasi-neutrality means that $n = p + 1$, where n and p are the electron and hole densities in the epilayer, both normalized to the doping level of the epilayer N_{epi} . We assume that there is no recombination in the epilayer, which gives a constant electron current. We also assume that there is no appreciable hole current. This implies that the hole quasi-Fermi level is constant. It equals the base voltage V_B . Using all these assumptions, the well-known 1-D drift-diffusion equations for electrons and holes can be integrated from $x = 0$ to $x = W_{\text{epi}}$. The result is

$$I_{\text{epi}} = (V_{CxCi} + V_{0W}) / R_{cV} \quad (2)$$

$$V_{0W} = V_T \left[2p_0 - 2p_W - \ln \left(\frac{1 + p_0}{1 + p_W} \right) \right]. \quad (3)$$

The epilayer current is now given in terms of the (normalized) hole densities p_0 and p_W at both ends of the epilayer. For the calculation of the hole densities we use the general relation $np = (n_i^2 / N_{\text{epi}}^2) \exp(V_{BC} / V_T)$ together with quasi-neutrality and find

$$p_0 = \frac{1}{2} \sqrt{1 + 4 \exp[(V_{BCi} - V_{ac}) / V_T]} - \frac{1}{2} \quad (4)$$

$$p_W = \frac{1}{2} \sqrt{1 + 4 \exp[(V_{BCx} - V_{ac}) / V_T]} - \frac{1}{2}. \quad (5)$$

The parameter V_{ac} is the built-in voltage of the base–epilayer junction and has the physical value $V_{ac} = V_T \ln(N_{\text{epi}}^2 / n_i^2)$.

For low injection, the hole density will be negligible compared to the doping level: $p \ll 1$. This means that $V_{0W} \simeq 0$. Hence, in this case, the epilayer current is simply the ohmic current through the epilayer, which has a resistance R_{cV} , defined in (1).

For high current densities, the transistor will go into quasi-saturation. Quasi-saturation means that the external base–collector bias is in reverse, or not too far in forward (say $V_{BCx} \lesssim 0.5$ V), but that the internal junction bias is almost as far in forward as the base–emitter junction ($V_{BCi} \gtrsim V_{ac}$). As can be seen from (4), the value of p_0 is then of the order of 1 or larger. Since there is now an exponential relation between V_{BCi} and the current I_{epi} , we can expect that V_{BCi} will remain at a value close to

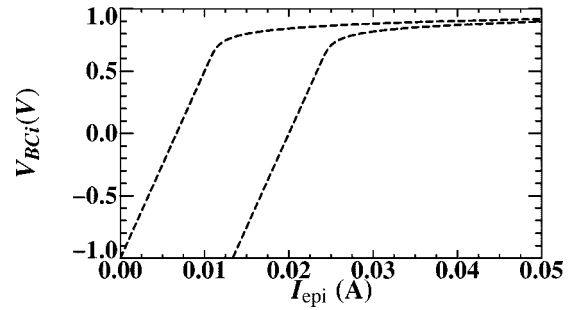


Fig. 2. The internal base–collector bias V_{BCi} as a function of the current I_{epi} for $V_{BCx} = -1, -3$ V. The parameters we used come from the experimental results of Section VII.

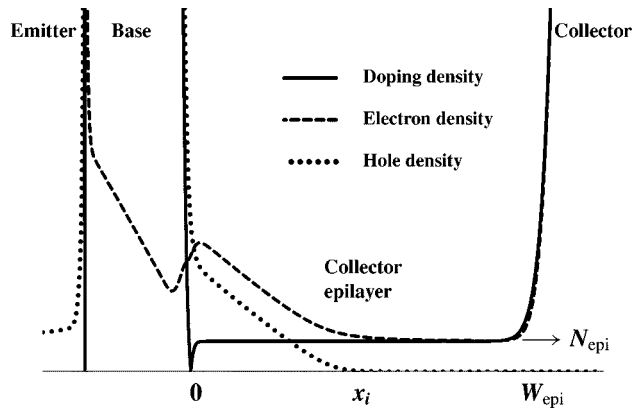


Fig. 3. Schematic view of the doping, electron, and hole densities in the base–collector region (on an arbitrary linear scale). It also shows the thickness of the epilayer W_{epi} and the injection layer x_i .

V_{ac} . To model the increase in current while the voltage difference $V_{CxCi} = V_{BCi} - V_{BCx}$ remains constant, the extra term V_{0W} / R_{cV} is present in (2).

In Fig. 2 we show the internal junction bias V_{BCi} as function of the current I_{epi} , where we keep the external bias V_{BCx} fixed. For low current densities, we see the ohmic region where V_{BCi} increases linear with the current. At some point quasi-saturation starts and the increase becomes very small. From then on, a small change in V_{BCi} results in a large change in p_0 , V_{0W} , and hence in I_{epi} .

In Fig. 3, we have shown on a linear scale the electron and hole densities in the collector epilayer, in the case of quasi-saturation. We can see that the epilayer consists of two parts. The first part, between $x = 0$ and x_i , is the injection region where the hole density is comparable to the electron density. The second part, between $x = x_i$ and W_{epi} , is the ohmic region where the hole density is negligible. At the point $x = x_i$, the difference between hole and electron quasi-Fermi levels is approximately $V_{BC}(x) \simeq V_{ac}$. We will use this observation in the next section for our improved model.

Within the framework of the Kull model, we can calculate the thickness of the injection region x_i . Since the voltage drop over the injection region is small, the voltage drop over the ohmic region is almost equal to the total voltage drop. This gives the relation

$$V_{BCi} - V_{BCx} = I_{\text{epi}} R_{cV} (1 - x_i / W_{\text{epi}}). \quad (6)$$

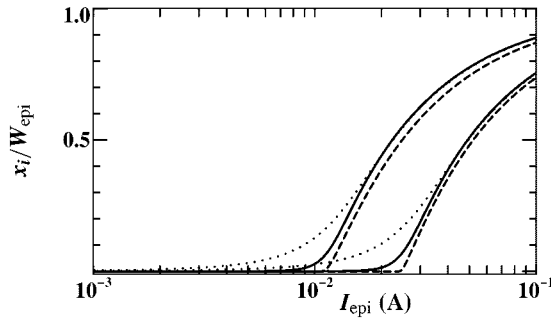


Fig. 4. The normalized thickness of the injection region x_i/W_{epi} as a function of the current I_{epi} for $V_{BCx} = -1, -3$ V. Dashed line: Kull model (6). Solid line ($a_{xi} = 0.1$) and dotted line ($a_{xi} = 0.3$): our model (10) (to be discussed later).

By using V_{BCi} here instead of V_{dc} the relation also holds for low current densities ($x_i \rightarrow 0$). We show x_i/W_{epi} as function of current in Fig. 4 (dashed line).

From Figs. 2 and 4, we observe that the Kull model has an abrupt onset of injection (this is the point where V_{BCi} becomes of the order of V_{dc} , or when x_i/W_{epi} starts to rise). This abrupt transition between the two operating regimes leads to poor modeling of the higher derivatives of the current. This can, for instance, be observed in low-frequency distortion analysis. It is especially this behavior that we want to improve.

In the original Kull model [1], velocity saturation was included, under the assumption, however, that the whole epilayer is quasi-neutral. The latter assumption no longer holds in modern transistors, in which the Kirk effect is important. Hence, even disregarding its abruptness, the original Kull model cannot be used for these transistors. In Section V, we will include velocity saturation in our model for the case where the epilayer does have a net charge.

IV. IMPROVEMENT OF THE KULL MODEL

To improve the formulation, we reverse the order of the calculations in the Kull model. For fixed external base–collector bias, we assume that the current I_{epi} is given, instead of the internal base–collector bias V_{BCi} . (See the appendix for a possible implementation.) From the current and from V_{BCx} , we calculate the thickness x_i of the injection region and from that the internal base–collector bias. The internal bias is used for further calculations of, for instance, the (reverse) main current in the base and the base charge, just as in other bipolar compact models.

A. Calculation of the Thickness x_i of the Injection Region

We use (6) to calculate the thickness of the injection region. But instead of using the voltage difference V_{BCi} at the junction itself, we use V_{dc} , which is the voltage difference at the end of the injection layer, as mentioned before. (Remember that both are almost the same, as long as there is injection: $x_i > 0$.) We can now write

$$\frac{x_i}{W_{\text{epi}}} = 1 - \frac{V_{\text{dc}} - V_{BCx}}{I_{\text{epi}} R_{\text{cv}}}. \quad (7)$$

In [4], a similar expression is used, but we will extend it to include velocity saturation effects in the next section. Equation (7) is only valid for currents that are sufficiently high to get the transistor into quasi-saturation. For any externally applied bias V_{BCx} , the current I_{qs} at the onset of quasi-saturation can be found from (7) by demanding that $x_i > 0$ when $I_{\text{epi}} > I_{qs}$. This results in

$$I_{qs} = \frac{V_{\text{dc}} - V_{BCx}}{R_{\text{cv}}}. \quad (8)$$

To use (7) also for currents below I_{qs} , we replace I_{epi} by \tilde{I}_{epi} where

$$\tilde{I}_{\text{epi}} = I_{qs} \frac{1 + a_{xi} \ln\{1 + \exp[(I_{\text{epi}}/I_{qs} - 1)/a_{xi}]\}}{1 + a_{xi} \ln\{1 + \exp[-1/a_{xi}]\}}. \quad (9)$$

Note that \tilde{I}_{epi} is always larger than I_{qs} , unless $I_{\text{epi}} = 0$, in which case $\tilde{I}_{\text{epi}} = I_{qs}$. This assures a nonnegative x_i . When $I_{\text{epi}} \gg I_{qs}$ we have $\tilde{I}_{\text{epi}} \simeq I_{\text{epi}}$, as desired. The dimensionless parameter a_{xi} has a smoothing purpose. Our experience is that it should be around 0.3 for Si homo-junction transistors, and possibly less for hetero-junction processes like SiGe.

The thickness of the injection region x_i is now calculated by solving

$$\tilde{I}_{\text{epi}} = \frac{V_{\text{dc}} - V_{BCx}}{R_{\text{cv}} (1 - x_i/W_{\text{epi}})} \quad (10)$$

for given V_{BCx} and I_{epi} . This equation, as well as the expression for I_{qs} , will be enhanced later on to include velocity saturation effects.

In Fig. 4, we have shown the results for x_i/W_{epi} , both for the original Kull model and for our improved model described above. Note that our model indeed shows a less abrupt onset of quasi-saturation than the Kull model. By changing a_{xi} , one can influence the abruptness by which x_i/W_{epi} , as function of the current, starts to increase.

B. The Internal Base–Collector Bias

Next we need to calculate the internal base–collector bias via the hole density p_0 . To this end, we combine (2) and (6) to obtain

$$\frac{x_i}{W_{\text{epi}}} I_{\text{epi}} R_{\text{cv}} = V_T \left[2p_0 - 2p_W - \ln \left(\frac{1 + p_0}{1 + p_W} \right) \right] \quad (11)$$

where the right-hand side is V_{0W} from (3). From this equation, we cannot calculate p_0 directly, since the equation does not yield an explicit expression for p_0 . We therefore approximate the equation above with

$$\frac{x_i}{W_{\text{epi}}} I_{\text{epi}} R_{\text{cv}} = 2V_T (p_0 - p_W) \frac{p_0 + p_W + 1}{p_0 + p_W + 2}. \quad (12)$$

The approximation for V_{0W} we just made does not differ more than 5% from the original equation for V_{0W} over the whole range of p_0 and p_W values. Using the second-order equation (12), we can now calculate p_0 from p_W , I_{epi} and x_i/W_{epi} . The internal base–collector bias can be found from (4) as

$$V_{BCi} = V_{\text{dc}} + V_T \ln[p_0 (p_0 + 1)]. \quad (13)$$

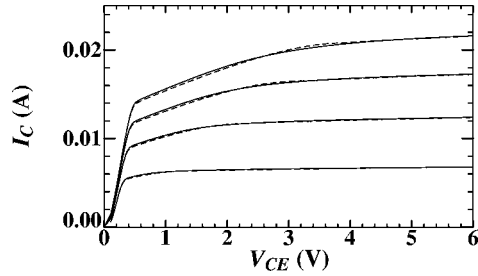


Fig. 5. Output characteristic for both the Kull model (dashed line) and our model (solid line) in the ohmic case. $I_B = 50 \mu\text{A}$, $100 \mu\text{A}$, $150 \mu\text{A}$, and $200 \mu\text{A}$.

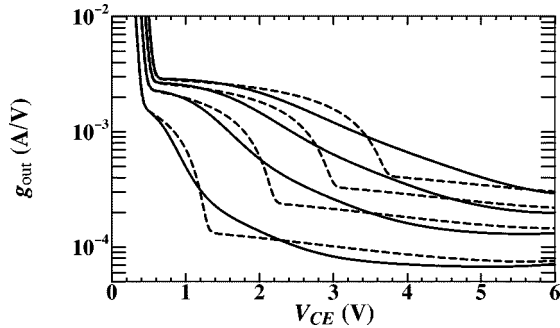


Fig. 6. Output conductance $g_{\text{out}} = dI_C/dV_{CE}$ corresponding to Fig. 5. Note the kink at the onset of quasi-saturation in the Kull model.

To compare results of different models for the collector epilayer, one needs to embed them in a complete compact model. The epilayer model described here (including velocity saturation effects described in the next section) is part of the new version 504 of Mextram. Keeping the rest of the model the same and changing only the model for the epilayer, we are able to give a realistic comparison between the Kull model (or the epilayer model of Mextram 503 [2]) and our new model.

The results for the output characteristics are given in Figs. 5 and 6 for the ohmic case. As one can see, the difference in the collector current is almost negligible. There is a much larger difference when we look at the output conductance. In the Kull model, one can see a kink when quasi-saturation sets in. In our new model, quasi-saturation is present also, but its onset is not as abrupt. We will see that the same holds for measurements. For higher derivatives, the difference between the two models becomes even larger.

V. VELOCITY SATURATION EFFECTS

The equations we presented above hold only when velocity saturation in the epilayer does not play a role. We will now include this in our description. For low electric field, the drift velocity of the electrons is proportional to the electric field: $v = \mu_n E$. For higher electric fields the velocity saturates. Its limiting value is the saturated drift velocity v_{sat} . We can estimate the currents for which velocity saturation becomes important by looking at the ohmic region (which has a constant electric field), and putting the drift velocity equal to the saturated drift velocity. The current we find is $I_{\text{hc}} = qN_{\text{epi}}A_{\text{em}}v_{\text{sat}}$. For epilayer currents of the order of I_{hc} or higher, velocity saturation effects need to be included.

In the original Kull model [1], velocity saturation is included, under the assumption, however, that the epilayer is quasi-neutral throughout. We will now show that when velocity saturation is important, this assumption no longer holds. At a current I_{hc} , the amount of electrons needed to sustain this current, assuming they are travelling at v_{sat} , is equal to the doping level. For even higher currents (or lower effective velocity), the electron concentration is even higher. These electrons have a negative charge, whereas the doping atoms provide a positive background charge. The net charge will no be longer negligible. With increasing current, the net charge will become negative. This has an effect on the electric field: it will not be constant anymore. Consequently, once velocity saturation needs to be taken into account ($I_{\text{epi}} \gtrsim I_{\text{hc}}$), the assumption of quasi-neutrality (and of a constant electric field) no longer holds. The net charge in the epilayer will eventually lead to the Kirk effect (also a form of quasi-saturation), which is important in many modern technologies. The Kull model is inadequate to describe the Kirk effect.

To include velocity saturation in our description, we will start with considering a very high current. Our approach is based on the same principles as those of [2]. From standard theory, we use the following two equations for the electric field:

$$\frac{dE}{dx} = \frac{qN_{\text{epi}}}{\epsilon} \left(1 - \frac{I_{\text{epi}}}{I_{\text{hc}}}\right) \quad (14)$$

$$\int_{x_i}^{W_{\text{epi}}} E dx = V_{BCx} - V_{\text{ac}}. \quad (15)$$

The electric field in the injection region can be neglected. As a boundary condition, we assume that the electric field at the end of the injection region is the critical electric field needed for velocity saturation:

$$E(x_i) = -v_{\text{sat}}/\mu_n = -I_{\text{hc}}R_{\text{cv}}/W_{\text{epi}} \quad (16)$$

where we used the low-field mobility. After a double integration of (14) and using (15), we get

$$V_{\text{ac}} - V_{BCx} = I_{\text{hc}}R_{\text{cv}}y_i + (I_{\text{epi}} - I_{\text{hc}})\text{SCR}_{\text{cv}}y_i^2. \quad (17)$$

Here $\text{SCR}_{\text{cv}} = W_{\text{epi}}^2/2\epsilon v_{\text{sat}}A_{\text{em}}$ is the space-charge resistance of the epilayer, i.e., the effective resistance of a region dominated by a current whose charge is not compensated by a background charge. We also abbreviated

$$y_i = \left(1 - \frac{x_i}{W_{\text{epi}}}\right). \quad (18)$$

Equation (17) is similar to (7) for the ohmic case. Now, however, we have described quasi-saturation due to the Kirk effect instead of due to an ohmic voltage drop. In both cases, we have a similar base widening and injection of holes into the epilayer.

We have to find an interpolation between the two cases of ohmic resistance and space charge resistance. We can use the same interpolation that has been used in [2, eq. (19)]. This implies replacing I_{hc} in (17) above by $I_{\text{hc}}I_{\Omega}/(I_{\text{hc}} + I_{\Omega})$, where the ohmic current is given by $I_{\Omega} = (V_{\text{ac}} - V_{BCx})/[R_{\text{cv}}(1 - x_i/W_{\text{epi}})]$. For high voltages over the epilayer, this will again

give I_{hc} , but for low voltages it will give the ohmic current we used in the previous section. The result is

$$I_{epi} = \frac{V_{dc} - V_{BCx}}{SCR_{Cv} y_i^2} \frac{V_{dc} - V_{BCx} + I_{hc} SCR_{Cv} y_i^2}{V_{dc} - V_{BCx} + I_{hc} R_{Cv}}. \quad (19)$$

Equation (19) can, as before, only be used for epilayer currents larger than I_{qs} , the current at the onset of injection. This is precisely the current when $x_i = 0$. We can find it directly from (19) resulting in

$$I_{qs} = \frac{V_{dc} - V_{BCx}}{SCR_{Cv}} \frac{V_{dc} - V_{BCx} + I_{hc} SCR_{Cv}}{V_{dc} - V_{BCx} + I_{hc} R_{Cv}}. \quad (20)$$

Next we follow the same procedure as we did for the ohmic case. Now that we have I_{qs} , we use (9) again for the definition of the current \tilde{I}_{epi} . We then replace I_{epi} in (19) by \tilde{I}_{epi} . This leads to a third-order equation for y_i . This equation can be solved and an explicit formula can be given. However, we have found that we can simplify it to a second-order equation without significant loss of accuracy. This is easier for the implementation in a circuit simulator and numerically more robust. Finally, we then find the following equation:

$$\tilde{I}_{epi} = \frac{V_{dc} - V_{BCx}}{SCR_{Cv} y_i^2} \frac{V_{dc} - V_{BCx} + I_{hc} SCR_{Cv} y_i}{V_{dc} - V_{BCx} + I_{hc} R_{Cv}}. \quad (21)$$

From this equation, we solve for y_i (or x_i).

Note that in the limit $I_{hc} \rightarrow \infty$ we get the ohmic result back from the previous section. In the other limit, $I_{hc} \rightarrow 0$, we get $\tilde{I}_{epi} = (V_{dc} - V_{BCx}) / [SCR_{Cv} (1 - x_i/W_{epi})^2]$. The relation between the current and the thickness of the injection region is now quadratic, instead of linear as in (10).

Using the thickness x_i , we calculate p_0 from (12) and the internal base-collector bias V_{BCi} from (13). Note that our description of the injection region ($x < x_i$) is not influenced by velocity saturation. This is caused by the fact that the carrier concentrations are high and the electric field is low, which means that the mobility has its low-field value.

VI. CURRENT SPREADING

The derivation we have given above contains the same physics as the Kull model [1] for the ohmic case or the previous Mextram model [2] when including velocity saturation. Up to now it is a one-dimensional model. To take current spreading into account the most important change is due to the fact that the three high current parameters no longer have their one-dimensional value. Instead they get an effective value. This effective value depends on the actual size of the emitter region in relation to the epilayer thickness. In [2] an example is given of the scaling of the high-current equations with geometry.

Current spreading as function of current can also be included. In [2, eq. (27)] it was shown how this can be done. We observed that in practice the current spreading as function of the epilayer current is of minor importance. Including it would mean solving a third order equation for y_i , something which we do not want (for numerical reasons), if it can be prevented. We therefore did not include this extra feature in our model.

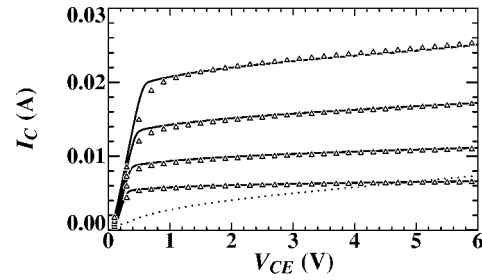


Fig. 7. Collector current for $I_B = 50 \mu\text{A}$, $100 \mu\text{A}$, $200 \mu\text{A}$, and $400 \mu\text{A}$. Markers are measurements, lines are the model. The dotted line shows the current I_{qs} , which is almost independent of the base current. For currents above I_{qs} the transistor is in quasi-saturation.

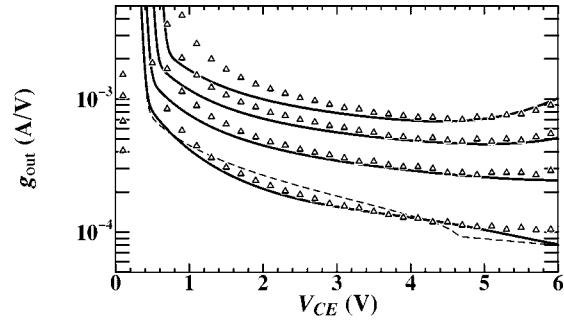


Fig. 8. Output conductance $g_{out} = dI_C/dV_{CE}$ corresponding to Fig. 7. The dashed curve shows the result from the old epilayer model for $I_B = 50 \mu\text{A}$. Note the kink at the point where the transistor goes into quasi-saturation.

VII. EXPERIMENTAL RESULTS

To compare our model with measurements, we present here results on a $0.6 \times 5.4 \mu\text{m}^2$ NPN-transistor from a 12-V BiCMOS process. The DUT contains five transistors in parallel. This transistor has been characterized completely (i.e., including temperature scaling) for the CMC benchmarking effort,⁴ together with five other transistors from various foundries, including two SiGe transistors. The extracted epilayer parameters for this high-voltage transistor are: $V_{dc} = 0.68 \text{ V}$, $R_{Cv} = 150 \Omega$, $SCR_{Cv} = 1250 \Omega$, $I_{hc} = 4 \text{ mA}$, and $a_{x1} = 0.3$.

Results of the output characteristics are shown in Figs. 7 (the current itself) and 8 (the derivative of the current, the output conductance). As one can see the current is modeled well, although the current densities are already high and beyond the normal operating range. Also the output conductance is described reasonably accurate. Only the transition to hard-saturation can still be improved. The observed differences are probably due to either current spreading, or to the fact that the hole current in the epilayer is no longer negligible.

In Fig. 7 we have also plotted I_{qs} , which does not depend very much on I_B . For the part of the curves higher than this dotted line, the transistor is in quasi-saturation (or hard saturation). For the lowest curve, the transition into quasi-saturation occurs at $V_{CE} \simeq 4.6 \text{ V}$. This transition can clearly be seen in the output conductance of the old model, see Fig. 8. Neither in the measurements nor in the new model do we see such a kink: the transition is much more smooth.

⁴For the Compact Model Council bipolar standardization effort, see <http://www.eigroup.org/cmc>

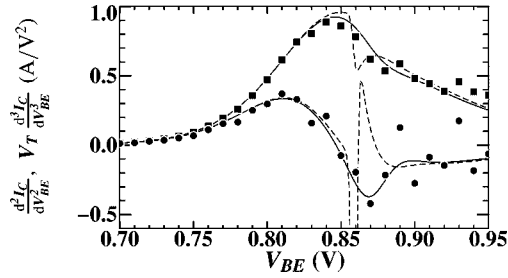


Fig. 9. The second (squares) and third (circles) derivative of the collector current w.r.t. V_{BE} in the Gummel plot, at $V_{BC} = 0$ V. The third derivative has been multiplied by V_T . The dashed lines are with the old epilayer model. The solid lines are our improved model.

Similar results are obtained if we look to the second and third derivative of the collector current in the Gummel plot (see Fig. 9). Here it is even more clear where the Kull model fails. We removed the large spikes in the derivatives of the old epilayer model, that can be seen around $V_{BE} \simeq 0.86$ V. The higher derivatives determine the low-frequency distortion behavior. For distortion at higher frequencies, the charge description also plays an important role [5].

VIII. THE EPILAYER CHARGE

For a complete description we also need an expression for the charge in the epilayer. To calculate it we use the Integral Charge Control Relation (ICCR) [6], [7] that is used in many models for the main current in the quasi-neutral base. It is expressed as

$$I_N = q^2 D_n A_{em}^2 n_i^2 (e^{V_{BE}/V_T} - e^{V_{BCi}/V_T}) / Q_B \quad (22)$$

where Q_B is the total hole charge from the base–emitter to the base–collector junction. Instead of taking only the base into account, we can also include the epilayer. The base charge must then be replaced by $Q_B + Q_{epi}$ and V_{BCi} must be replaced by V_{BCx} . Subtracting both equations gives the total hole charge in the epilayer

$$Q_{epi} = q^2 D_n A_{em}^2 n_i^2 (e^{V_{BCi}/V_T} - e^{V_{BCx}/V_T}) / I_{epi}. \quad (23)$$

The pre-factor $q^2 D_n A_{em}^2 n_i^2$ contains the diffusion constant D_n and intrinsic carrier concentration n_i of the collector epilayer. As long as these quantities are almost equal to those in the base [8], the pre-factor in (23) can be given in terms of parameters of the intrinsic model, for instance, $I_s \times Q_{B0}$, and we do not need an extra parameter. In cases where there is a large difference in, for instance, n_i between the collector epilayer and the base (as in SiGe-processes [9]), we do need an extra parameter (see below).

We can rewrite (23) using (4), (5), and (12) to get an expression for Q_{epi} directly in terms of hole densities, such that it can be used also when $I_{epi} = 0$

$$Q_{epi} = \tau_{epi} \frac{2V_T}{R_{cv}} \frac{x_i}{W_{epi}} (p_0 + p_W + 2) \quad (24)$$

$$\tau_{epi} = I_s Q_{B0} \left(\frac{R_{cv}}{2V_T} \right)^2 e^{V_{ac}/V_T} = \frac{W_{epi}^2}{4D_n}. \quad (25)$$

Flexibility in parameter extraction is enhanced when τ_{epi} is made a model parameter itself, instead of being a function of DC parameters. As mentioned before, for SiGe-processes we

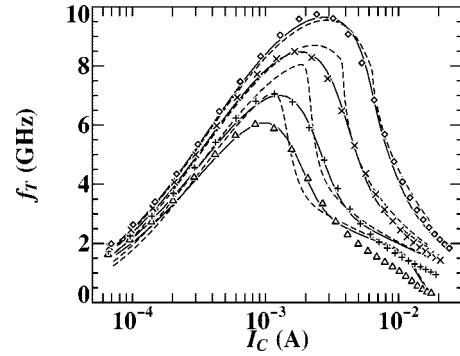


Fig. 10. Cutoff frequency f_T for $V_{CE} = 0.5, 0.8, 2.0, 5.0$ V (bottom to top). Markers are measurements, solid lines are from the new epilayer model, and dashed lines are from the old epilayer model.

even need the extra parameter τ_{epi} . [The first expression in (25) for τ_{epi} then needs refinement.]

In quasi-saturation the hole charge p_W at the interface of epilayer and buried layer may be neglected. The expression for the epilayer charge (24) then becomes, using again (12)

$$Q_{epi} \simeq \tau_{epi} \left(\frac{x_i}{W_{epi}} \right)^2 I_{epi}. \quad (26)$$

This equation was first given in [10] and is used in the compact model Hicum [4].⁵ Rather than (26), we use the full expression (24) for the charge because it also describes the charge in the case of hard saturation (where the current is small but the charge is not) as well as in reverse mode of operation.

From (22) and (23), it seems logical to make a description where the main current is given in terms of the biases V_{BE} and V_{BCx} and the total hole charge $Q_B + Q_{epi}$. There are three reasons why we prefer not to do this. First, we now have a current model independent of the epilayer charge model. This means that the parameter τ_{epi} can be used freely to get a better description of the cutoff frequency. Second, (22) and (23) hold for a one-dimensional transistor. They do not include current spreading effects, which can be very important in the epilayer. By having a parameter available for the epilayer charge that has no influence on the currents we can keep these effects separated. Third, by describing the base and the collector epilayer separately, we have a more natural description of SiGe-base/Si-collector transistors. We do not need to include extra charge enhancement factors [11] to be able to use the ICCR simultaneously in the base and in the epilayer. Instead, we use it twice, once for each region, with separated parameters.

With the expression for the charge, we can calculate the cutoff frequency f_T , shown in Fig. 10. The cutoff frequency f_T is related to the total transit time $\tau_T = dQ/dI_C$. Since in the old epilayer model the collector current is not very smooth (as can be seen from the abruptness in its first derivative g_{out}), one cannot expect the cutoff frequency to be smooth either. This can indeed be observed in the plot of f_T , which shows a clear kink in the previous model when the transistor goes into quasi-saturation. It must be mentioned that this specific transistor has been chosen for the problems it poses for modeling the epilayer and that the

⁵For the model definition and more information about Hicum, see http://www.iee.et.tu-dresden.de/iee/eb/comp_mod.html

f_T -result is not representative for the previous model (Mextram 503). The new model shows a clear improvement. Obviously such a better description also facilitates parameter extraction.

IX. TEMPERATURE SCALING

The temperature scaling of the parameters of the high-current regime is rather easy. The diffusion voltage V_{dc} scales as any diffusion voltage in most, if not all, bipolar compact models, and needs one temperature parameter: a bandgap voltage. The parameters I_{hc} and SCR_{cv} do not scale with temperature. The variation of low-current resistance R_{cv} with temperature is determined by the temperature variation of the mobility. We therefore have $R_{cv} \sim T^{A_{epi}}$, where A_{epi} is the temperature parameter and T the absolute temperature. When the doping level of the epilayer is known, this parameter can be found from the temperature dependence of the electron mobility at that doping level. For the transit time of the epilayer we find $\tau_{epi} \sim T^{A_{epi}-1}$, since the transit time goes with the diffusion constant [see (25)].

X. PARAMETER EXTRACTION

Parameter extraction is an important issue in the use of a compact model. For many of the Mextram model parameters, standard methods can be used. This includes the depletion capacitances and other low-current parameters like those of the forward and reverse Early effect, avalanche multiplication, and the collector, base, and substrate saturation currents. Also for the extraction of the resistances of base, emitter, and collector buried layers, standard methods can be applied. Here we need to be concerned only with the parameters discussed in this paper, that is, the parameters related to the series resistance of the collector epilayer.

In general, the extraction of parameters related to high-current operation of a bipolar transistor is complex. This complexity is even enhanced due to self-heating at high currents. To take into account self-heating, we need to know the parameters for temperature scaling. Fortunately, the most important temperature parameters can be extracted from measurements at small current densities performed at various temperatures. From the decrease of the base-emitter voltage in the output characteristic (I_C versus V_{CE} at constant I_B), the rise of the temperature can be estimated.

The Mextram model mainly distinguishes itself from other compact models like Vbic and Hicum in the way the collector epilayer resistance is modeled. However, since the basic physics are the same, all models have similar parameters. Hence similar parameter extraction methods can be used. Our preferred method is discussed below. In all cases one should start with good initial values. These can be calculated when the dimension of the emitter and the thickness and doping level of the epilayer are known. Since the parameters have a physical meaning, their optimized values should not be far from the initial values.

Next, one needs to know how the parameters influence the characteristics. The parameters R_{cv} , SCR_{cv} and I_{hc} determine the onset of quasi-saturation. Parameter V_{dc} determines the increase of the injection layer thickness with collector current. The effect of R_{cv} and V_{dc} can be seen predominantly in the decrease of the DC gain with collector current at small (zero) base-collector

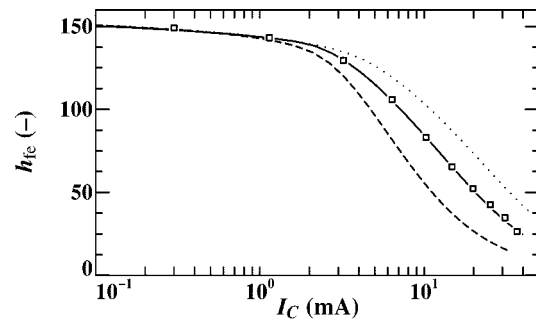


Fig. 11. The dc current amplification as function of the collector current for $V_{BC} = 0$ V. The markers are the measurements. The lines are simulations for various values of the low-current epilayer resistance: $R_{cv} = 150 \Omega$ (solid), $R_{cv} = 75 \Omega$ (dotted), and $R_{cv} = 300 \Omega$ (dashed).

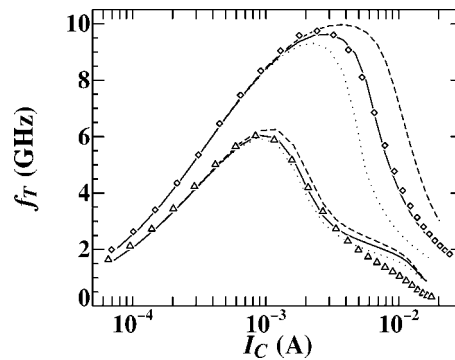


Fig. 12. The cutoff frequency f_T as function of the collector current for $V_{CE} = 0.5$ V (triangles) and 5.0 V (diamonds). The markers are the measurements from Fig. 10. The lines are simulations for various values of the epilayer space-charge resistance: $SCR_{cv} = 1250 \Omega$ (solid, as in Fig. 10), $SCR_{cv} = 625 \Omega$ (dotted), and $SCR_{cv} = 2500 \Omega$ (dashed).

voltage. We have shown the effect of varying R_{cv} in Fig. 11. Therefore the Gummel plot measured at $V_{BC} = 0$ V (which is only slightly influenced by self-heating) is used to extract both parameters. Nevertheless, R_{cv} and V_{dc} are to some extent correlated, and it is difficult to extract both in a unique way. This is not needed, since V_{dc} is mainly determined by the doping level and is therefore more or less geometry-independent. It can be fixed at the calculated value, depending on the specific bipolar process, whereas R_{cv} can then be optimized.

It is hard to extract I_{hc} and SCR_{cv} from the decrease of the dc gain measured at higher collector voltages. Often avalanche multiplication, self-heating, and high injection in the base (modeled by a knee current) determine the gain. The knee current can be extracted from I_C in the output characteristic at sufficient high collector voltage where the transistor is not in quasi-saturation and avalanche multiplication not yet present. The DC gain is then modeled well over the entire collector current and voltage range.

From the cutoff frequency f_T we extract the other high-current parameters. The transit time parameters of the base and emitter determine the maximum of f_T . The onset of quasi-saturation (the current where f_T decreases rapidly) is set by I_{hc} and SCR_{cv} . In Fig. 12 we have shown the influence of SCR_{cv} on the cutoff frequency. Note that it is mainly for the larger currents that SCR_{cv} is important, whereas R_{cv} is important for the lower current densities. By changing I_{hc} one has a way of determining where the transition between the two parameters takes

TABLE I
CONVERGENCE RESULTS

#	Circuit		#Iterations	
	#unknowns	#Mextram	503	504
1	470	42	181	181
2	238	13	TR	166
3	116	7	247	207
4	174	12	153	153
5	2758	260	316	312
6	2962	288	772	319
7	626	32	203	165
8	3900	264	TR	346
9	130	11	TR	TR
10	1562	156	254	266
11	1211	150	332	335
12	10	1	TR	34

place. The transit time of the epilayer τ_{epi} determines mainly the cutoff frequency when the transistor is in deep quasi-saturation ($Q_{\text{epi}} > Q_B + Q_E$).

XI. CONVERGENCE RESULTS

The new epilayer model has been implemented, amongst others, in our in-house circuit simulator Pstar (see the Appendix for some implementation issues). The simulator has been used to do some convergence tests. These tests were based on twelve different circuits of real designs for filters, bandgap references, high-gain amplifiers, and picture correction circuits. They were designed for various processes (and hence with various parameter sets), like pure bipolar, BiCMOS and DMOS processes. The results are shown in Table I. The total number of unknowns (node voltages) as well as the number of bipolar instances (modeled with Mextram) is given. The last two columns show the number of iterations the simulator needed, both for Mextram 503 (with the old epilayer model) and Mextram 504 (with the new model discussed here). The Mextram 504 parameters were automatically calculated from the Mextram 503 ones. TR stands for cases where direct convergence was not reached and the simulator had to go to transient methods for convergence. As one can see, the new model gives similar or (much) better results for convergence.

XII. SUMMARY

We have given a compact model for the behavior of the collector epilayer of a bipolar transistor. It includes base-widening and quasi-saturation due to an ohmic voltage drop as well as due to the Kirk effect. The excess charge is also described.

We have shown that compared to, for instance, the Kull model it gives a much smoother behavior, which can already be seen in the first derivatives like g_{out} and f_T . Smoothness is particularly important for higher derivatives which determine the distortion behavior. The new model is in very good agreement with experiments. This holds for those described here as well as for measurements from many other transistors, including state-of-the-art double-poly transistors and various SiGe ones. It also shows good convergence behavior in practical circuits.

The epilayer model is part of a new Mextram 504 release, and can be implemented also in other models.

APPENDIX IMPLEMENTATION ISSUES

In this appendix, we will give some remarks about the actual implementation of our model into a circuit simulator.

In forward mode we calculated the internal base-collector bias V_{BCi} as function of the bias V_{BCx} and the current I_{epi} . In many circuit simulators, however, the node voltages are given and the currents need to be calculated. To circumvent this problem we start with the biases as given by the circuit simulator (*cs*): V_{BCx} and $V_{BCi,cs}$. From these we calculate in some way the current I_{epi} (see below). Using this current we calculate V_{BCi} , as described in the main text. The bias V_{BCi} (and not $V_{BCi,cs}$) is then used to calculate other quantities like the main current I_N in (22) and base charges.

In principle, we can take any expression for the current as function of V_{BCx} and $V_{BCi,cs}$, since in forward mode we only need it as a kind of ‘‘current sensor.’’ In practice, it is convenient to take the same expression as the one we use in reverse mode of operation. In reverse, the epilayer will be flooded with electrons (since the base-collector junction is in forward). The electric fields will be low and therefore velocity saturation is not important. As a result the Kull model can be used to describe the current in reverse. (Note that there is no transition to quasi-saturation, for which we need to consider the abruptness.) Therefore, we take the original Kull formulation (with $V_{BCi,cs}$ instead of V_{BCi}) for the calculation of the current I_{epi} , both in reverse and in forward.

To make sure that the forward mode and reverse mode give continuous results around $I_{\text{epi}} = 0$ we must make sure that x_i is continuous there. We can calculate from the Kull model that $x_i = p_0/(1 + p_0) = p_W/(1 + p_W)$ for zero current. To make sure that we get the same result in forward mode we take $x_i = 1 - y_i/(1 + p_W y_i)$, instead of $x_i = 1 - y_i$ as previous defined. (Note that $y_i = 1$ when $I_{\text{epi}} = 0$.) This does not influence the normal forward mode of operation where $p_W \simeq 0$.

We have discussed the normal forward operation, as well as the reverse mode of operation. As a final point we need to consider the transition from normal forward operation or quasi-saturation to hard saturation. In the latter case not only V_{BCi} is of the order of V_{dc} , but also V_{BCx} . In the main text we have used the expression $V_{\text{dc}} - V_{BCx}$. We cannot allow this to become negative and therefore replace it by

$$V_{qs} = \frac{1}{2} \left(V_{qs}^{\text{th}} + \sqrt{(V_{qs}^{\text{th}})^2 + 0.04V_{\text{dc}}^2} \right) \quad (27)$$

where V_{qs}^{th} is the theoretical value $V_{\text{dc}} - V_{BCx}$.

Using the expression above, the transistor will go into hard saturation when $V_{qs}^{\text{th}} \simeq 0$, or when $V_{BCx} \simeq V_{\text{dc}}$. We have noticed that, especially for large currents, this is a bit too early. (One can only observe this when considering the simulated output conductance in detail.) We have found that it helps to write instead $V_{qs}^{\text{th}} = V_{BCi}^{(\text{appr})} - V_{BCx}$, where

$$V_{BCi}^{(\text{appr})} = V_{\text{dc}} + 2V_T \ln \left(\frac{I_{\text{epi}} R_{\text{cv}}}{2V_T} + 1 \right) \quad (28)$$

is the approximate value of V_{BCi} in quasi-saturation (but not hard saturation). It can be found from (12) and (13) by taking $x_i/W_{epi} = 1$ and assuming $p_0 \gg 1$ and $p_0 \gg p_W$.

ACKNOWLEDGMENT

The authors would like to thank M. Stoutjesdijk for doing the convergence tests.

REFERENCES

- [1] G. M. Kull, L. W. Nagel, S. Lee, P. Lloyd, E. J. Prendergast, and H. Dirks, "A unified circuit model for bipolar transistors including quasisaturation effects," *IEEE Trans. Electron Devices*, vol. ED-32, pp. 1103–1113, June 1985.
- [2] H. C. de Graaff and W. J. Kloosterman, "Modeling of the collector epilayer of a bipolar transistor in the Mextram model," *IEEE Trans. Electron Devices*, vol. 42, pp. 274–282, Feb. 1995.
- [3] C. C. McAndrew, J. A. Seitchik, D. F. Bowers, M. Dunn, M. Foisy, I. Getreu, M. McSwain, S. Moinian, J. Parker, D. J. Roulston, M. Schröter, P. van Wijnen, and L. F. Wagner, "Vbic95, the vertical bipolar intercompany model," *IEEE J. Solid-State Circuits*, vol. 31, pp. 1476–1483, 1996.
- [4] M. Schröter and T.-Y. Lee, "Physics-based minority charge and transit time modeling for bipolar transistors," *IEEE Trans. Electron Devices*, vol. 46, pp. 288–300, 1999.
- [5] M. Schröter, D. R. Pehlke, and T.-Y. Lee, "Compact modeling of high-frequency distortion in bipolar transistors," in *ESSDERC*, vol. 29, 1999, pp. 476–479.
- [6] J. L. Moll and I. M. Ross, "The dependence of transistor parameters on the distribution of base layer resistivity," *Proc. IRE*, vol. 44, pp. 72–78, Jan. 1956.
- [7] H. K. Gummel, "A charge control relation for bipolar transistors," *Bell Sys. Tech. J.*, pp. 115–120, Jan. 1970.
- [8] D. B. M. Klaassen, J. W. Slotboom, and H. C. de Graaff, "Unified apparent bandgap narrowing in *n*- and *p*-type silicon," *Solid-State Electron.*, vol. 35, no. 2, pp. 125–129, 1992.
- [9] H. Kroemer, "Two integral relations pertaining to the electron transport through a bipolar transistor with a nonuniform energy gap in the base region," *Solid-State Electron.*, vol. 28, pp. 1101–1103, 1985.
- [10] J. R. A. Beale and J. A. G. Slatter, "Equivalent circuit of a transistor with a lightly doped collector operating in saturation," *Solid-State Electron.*, vol. 11, pp. 241–252, 1968.
- [11] M. Schröter, M. Friedrich, and H.-M. Rein, "A generalized integral charge-control relation and its application to compact models for silicon-based HBT's," *IEEE Trans. Electron Devices*, vol. 40, pp. 2036–2046, 1993.



Jeroen C. J. Paasschens was born in Valkenswaard, The Netherlands, in 1970. He received the M.Sc. degree in physics from the University of Nijmegen, The Netherlands, in 1994, and the Ph.D. degree from the University of Leiden, The Netherlands, in 1997.

He joined Philips Research Laboratories, Eindhoven, in 1998, and has been working on bipolar device modeling for circuit simulation. He is currently a member of the Modeling and Characterization Program committee of the Bipolar/BiCMOS Circuits and Technology Meeting (BCTM).



Willy J. Kloosterman was born in Olst, The Netherlands, in 1951. He graduated from the Technical College in Zwolle in 1974.

He joined Philips Research Laboratories Eindhoven, The Netherlands, in 1974. He worked on the dynamical behavior of CRT tubes, powder compaction models, and, since 1980, has been involved in bipolar and MOS compact transistor modeling, characterization, and parameter extraction. In 2001 he joined Philips Semiconductors, Nijmegen, The Netherlands, where he works on

process characterization.



Ramon J. Havens was born in Nijmegen, the Netherlands, in 1972. He graduated from the Eindhoven Polytechnic, The Netherlands, in 1995.

He joined Philips Research Laboratories Eindhoven, The Netherlands, in 1996. He has been involved in bipolar characterization and high-frequency measurements.



Henk C. de Graaff was born in Rotterdam, The Netherlands, in 1933. He received the M.Sc. degree in electrical engineering from the Delft University of Technology, Delft, The Netherlands in 1956, and the Ph.D. degree from the University of Technology, Eindhoven, The Netherlands in 1975.

He joined Philips Research Laboratories, Eindhoven, in 1964, and has been working on thin film transistors, MOST, bipolar devices, and material research on polycrystalline silicon. His present field of interest is device modeling for circuit simulation.

Since his retirement from Philips Research (Nov. 1991) he has been consultant to the University of Twente (until 1996) and the Technical University of Delft, both in The Netherlands.